THE JOURNAL OF PHYSICAL CHEMISTRY A

ARTICLE

pubs.acs.org/JPCA

Influence of External Force on Properties and Reactivity of Disulfide Bonds

Maria Francesca Iozzi,* Trygve Helgaker, and Einar Uggerud

The Center for Theoretical and Computational Chemistry (CTCC), Department of Chemistry, University of Oslo, P.O. Box 1033, Blindern, N-0315 Oslo, Norway

Supporting Information

ABSTRACT: The mechanochemistry of the disulfide bridge—that is, the influence of an externally applied force on the reactivity of the sulfur−sulfur bond—is investigated by unrestricted Kohn−Sham theory. Specifically, we apply the COGEF (constrained geometry simulates external force) approach to characterize the mechanochemistry of the disulfide bond in three different chemical environments: dimethyl disulfide, cystine, and a 102-atom model of the I27 domain in the titin protein. Furthermore, the mechanism of the thiol−disulfide reduction reaction under the effect of an external force is investigated by considering the COGEF potential for the adduct and transition-state clusters. With the unrestricted Becke−three-parameter−Lee−Yang−Parr (UB3LYP) exchange−correlation functional in the 6-311++G(3df,3pd) orbital basis, the rupture force of dimethyl disulfide is 3.8 nN at a disulfide bond elongation of 35 pm. The interaction with neighboring groups and the effect of conformational rigidity of the protein environment have little influence on the mechanochemical characteristics. Upon stretching, we make the following observations: the diradical character of the disulfide bridge increases; the energy difference between the singlet ground state and low-lying triplet state decreases; and the disulfide reduction is promoted by an external force in the range 0.1−0.4 nN. Our model of the interplay between force and reaction mechanism is in qualitative agreement with experimental observations.

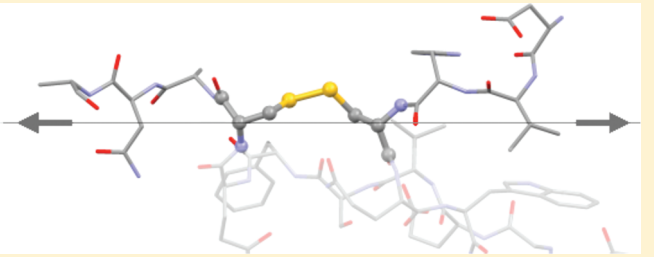

INTRODUCTION

The disulfide bond is found in many proteins, where it cross-links peptide chains—for example, in insulin.[1] By imposing constraints on protein folding, the disulfide link has a direct influence on the tertiary structure and consequently on protein function (shape, rheology, enzyme action). Interestingly, nature has developed strategies for fast responses to changes in the environment by the activation or deactivation of protein functions. The efficiency of these responses relies on rapid disulfide formation and scission mechanisms[2] in the formal redox reaction:

$$R-S-S-R' \rightleftharpoons R-S-H + R'-S-H$$

Apart from chemical stress, biological macromolecules are subject to mechanical influence from the surroundings; conversely, they may act on their surroundings by performing work—for example, muscle contraction. Importantly, the structure and chemical properties of a molecule change under the influence of an external force, giving rise to the concept mechanochemistry—a diverse field of chemistry that includes the study of polymer elasticity, sonochemical reactions, and force-induced changes in spectroscopic parameters.[3,4] Some of these ideas have recently received attention through atomic-force-microscopy (AFM) experiments.[5] In such experiments, a polymer is positioned between the cantilever tip and the base of the AFM apparatus. Molecular stretching is subsequently induced by applying tension to the cantilever. In 1999, Grandbois et al.[6] demonstrated that a covalent bond can be ruptured in this way.[7−10]

The synergy between chemical and mechanical forces on the muscle protein titin has been studied by Fernandez et al.[11−13] These authors applied a stretching force to an engineered molecule containing the titin I27 domain, whose folded structure is influenced by a disulfide bridge. By means of AFM, they were able to unfold the protein in a controlled fashion so that the disulfide bridge, initially protected inside the I27 domain, becomes exposed to the surrounding solution.[14,15] It was observed that, with a suitable reduction agent present, the applied force accelerates the reactive processes leading to disulfide cleavage.[16−19] The protein unfolding and S−S bond reduction have been modeled by molecular-mechanics[11,12,19−23] and quantum-chemical[17] simulations.

To a first approximation, the force-modified potential-energy surface can be regarded as a Born−Oppenheimer surface of reduced dimension, arising from the constraints imposed by the applied force. Indeed, several computational models are based on this idea. In particular, Beyer introduced the concept of a COGEF

Received: October 1, 2010
Revised: January 18, 2011
Published: March 02, 2011

(Constrained Geometry simulates External Force) path,[24] along which the distance between the two end atoms is increased in a stepwise fashion, relaxing the geometry at each step with respect to all remaining degrees of freedom. Recently, Wolinski et al.[25] proposed an alternative approach—rather than setting up an internal force by stretching the molecule, an external force is applied to selected nuclei, thereby inducing bond elongation. A number of similar approaches have been developed to study the potential-energy surfaces of force-induced chemical reactions, including those of Ribas-Arino et al.,[26,27] Ong et al.,[28,29] and Kucharski et al.[30]

In the present study, we apply the COGEF approach to study the mechanochemical properties of the disulfide bond in three different chemical systems, correlating the force-induced changes in the molecules with those in the electronic structure. In the first part of this study, we investigate the mechanical stretching of disulfide bonds in molecules of different sizes (dimethyl disulfide, cystine, and a small model of the titin I27 domain) to examine the role of the molecular environment—more specifically, to determine whether disulfide bonds in small molecules are useful models of disulfide bridges in proteins. In the second part, we study how the application of an external stretching force influences the susceptibility of the disulfide bond toward chemical reducing agents, focusing on the relationship between the direction and magnitude of the force relative to the reaction coordinate of the reduction reaction.

COMPUTATIONAL DETAILS

The mechanochemical characteristics of a molecule are conveniently described in terms of the changes that occur in energy and structure along the COGEF path, from the unperturbed equilibrium geometry toward the fully separated atoms via the *breaking point*—that is, the inflection point, where the force assumes its maximum value known as the *rupture force*. In a previous publication, we demonstrated that single-configuration-based electronic-structure methods are sufficient for describing mechanochemistry, noting that the breaking point occurs well before the transition structure is reached. In agreement with this observation, we found that most popular exchange−correlation functionals of Kohn−Sham theory are adequate for mechanochemical studies.[31] The exchange−correlation functionals used in the present work were benchmarked for ground-state properties as well as for the mechanochemical characteristics of dimethyl disulfide—see Tables 1−4 of the Supporting Information and ref 31. As shown by comparison with CCSD(T) theory, hybrid Kohn−Sham theory provides a good representation of the COGEF path up to bond rupture.[31]

In this work, we have used the unrestricted Becke−three-parameter−Lee−Yang−Parr (UB3LYP) hybrid functional to study the mechanochemical properties of CH_3SSCH_3, of cystine, and of a small model of the titin I27 domain referred to as titin-$I27_{SS}$; see the Supporting Information. To reduce cost, the cystine 2D-COGEF was computed with the unrestricted Becke−Perdew-86 functional of the generalized-gradient approximation (GGA). As already observed in our previous work,[31] the mechanochemical characteristics computed with GGA and hybrid functionals agree to within the experimental accuracy. We used the 6-311++G(3df,3pd) basis for CH_3SSCH_3 and the 6-31g(d) basis for the other molecules (and for comparisons among the molecules). To reduce cost, the cystine 2D-COGEF was computed with the resolution-of-identity (RI) technique.[32] For titin-$I27_{SS}$, the RI technique was used for conformational prescreening, whereas the full COGEF optimization was done without the RI technique. All non-RI calculations were carried out with Gaussian03,[33] whereas the RI calculations were performed with Turbomole.[34]

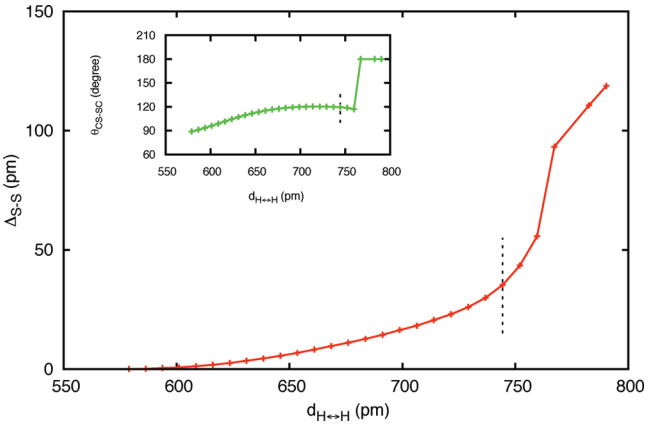

Figure 1. Stretching the CH_3SSCH_3: the S−S bond length d_{SS} and the CS−SC torsional angle θ as functions of the applied elongation. The vertical dashed lines indicate the breaking point. The COGEF path, calculated at the UB3LYP/6-311++G(3df,3pd) level of theory, has a breaking point at 241 pm corresponding to a rupture force of 3.8 nN.

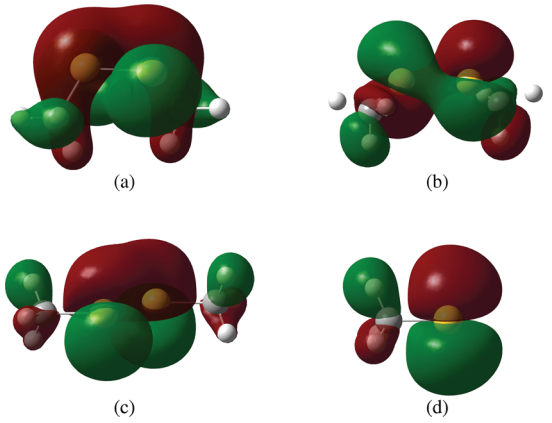

Figure 2. HOMO of CH_3SSCH_3 at selected points along the GOGEF path: (a) at the equilibrium geometry d_{SS} = 205 pm, (b) at the breaking point d_{SS} = 241 pm, (c) beyond the breaking point d_{SS} = 299 pm, (d) for the free CH_3S radical. The COGEF path was computed at the UB3LYP/6- 311++G(3df,3pd) level of theory.

RESULTS

Dimethyl Disulfide Stretching. The stretching of CH_3SSCH_3 was modeled by stepwise increasing the distance between the terminal hydrogen atoms $d_{H\leftrightarrow H}$ at the UB3LYP/6-311++G-(3df,3pd) level of theory. The main structural changes along the COGEF path are the S−S bond stretching (d_{SS}) and CS−SC torsional motion (θ), see Figure 1. At the early stage of the stretching with $\Delta_{H\leftrightarrow H} = d_{H\leftrightarrow H} - d^{eq}_{H\leftrightarrow H} < 100$ pm, d_{SS} increases smoothly, while θ twists from 90° to 120°. For 70 pm < $\Delta_{H\leftrightarrow H}$ < 100 pm, the molecule loses its torsional flexibility, and further stretching results in a pronounced elongation of the S−S bond. Bond rupture occurs at $\Delta_{H\leftrightarrow H}$ = 171 pm, where the S−S and C−S bonds have increased by 35 and 14 pm, respectively, showing that bond angle and torsional angle deformations contribute strongly

dx.doi.org/10.1021/jp109428g |J. Phys. Chem. A 2011, 115, 2308–2315

to the total elongation. Beyond the breaking point, S−S bond elongation is the only significant change observed, leading to the formation of two $CH_3S^{\bullet}$ fragments. To get some insight into the bond breaking induced by the external force, we have in Figure 2 plotted the highest occupied molecular orbital (HOMO) of CH_3SSCH_3. As these plots demonstrate, bonding is progressively lost upon stretching. Beyond bond rupture, the HOMO becomes increasingly localized, and a biradical character can be inferred by comparing with the HOMO of the isolated $CH_3S^{\bullet}$ radical in Figure 2d. Localization of the electron density on atoms and fragment groups is observed also in the Mulliken atomic charges of Table 3 in the Supporting Information: at equilibrium, the sulfur atoms possess small positive charges, which become increasingly less positive upon stretching.

The increased radical character of CH_3SSCH_3 induced by the applied force has another consequence, since it may promote intersystem crossings between the singlet ground state (S) and low-lying triplet states as the energy separations become sufficiently small along the COGEF path.[35−37] We were able to identify two such triplet states, close in energy but of different structures. The T1 state has an eclipsed C_{2v} cis structure with an S−S bond length of 267.5 pm, whereas the T2 state has a staggered C_{2h} anti structure with an S−S bond length of 254.4 pm. At equilibrium, the T1 and T2 states are close in energy and well separated from the ground state (by 208 and 194 kJ/mol, respectively), see Table 1. As the force is applied, the S and T2 states approach each other (see Figure 3), crossing beyond the breaking point. At the breaking point, the molecular structures are similar, indicating an efficient mechanism for force-induced singlet−triplet spin flipping. Interestingly, it was recently demonstrated experimentally that the stretching of a molecule by AFM may affect its magnetism.[38]

Table 1. Comparison of Singlet Ground-State (S) Structure, Lowest-Lying Triplet Structures (T1 and T2), and the Breaking-Point Structure of CH_3SSCH_3, Calculated at the UB3LYP/6-311++G(3df,3pd) Level of Theory

CH_3SSCH_3	S	T1	T2	breaking point
θ (°)	87	0	177	119
d_{SS} (pm)	205.3	263.7	257.0	240.6
ΔE (kJ/mol)	0	208	194	211

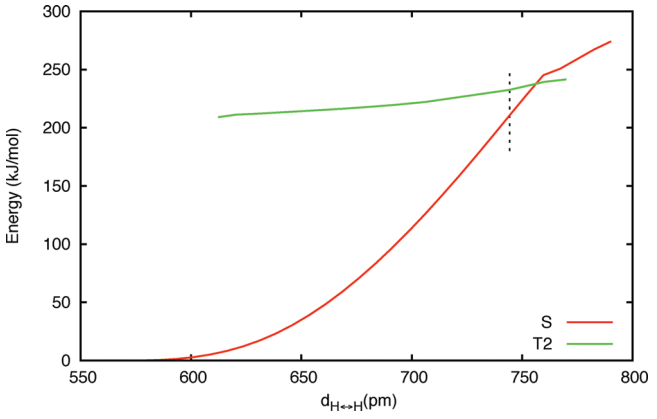

Figure 3. COGEF paths of the singlet S and triplet T2 states of CH_3SSCH_3, calculated at the UB3LYP/6-311++G(3df,3pd) level of theory. The dashed vertical line indicates the breaking point.

Cystine Stretching. Cystine is the dimer of *l*-cysteine *CH(COOH)(NH_2)CH_2SH in Figure 4, with the two moieties linked by a disulfide bond. It serves as a small model that incorporates many of the essential features of a protein disulfide link. Starting from the geometry-optimized structure, the UB3LYP/6-31G(d) COGEF path was computed by increasing the separation $d_{C^*\leftrightarrow C^*}$ between the two chiral carbon atoms in a stepwise manner. At the early stages of the stretching, the CS−SC dihedral angle θ increases from 90°, and the molecule progressively loses its conformational flexibility. At a dihedral angle of about 120°, the sulfur atoms begin to move apart, reaching the breaking point ($\Delta_{C^*\leftrightarrow C^*}$ = 190 pm and θ = 120°) after an elongation of 34 pm. We also observe a less pronounced stretching of the first-neighboring S−C bonds and second-neighboring C−C* bonds—in fact, at the breaking point, they have undergone an elongation of 12 and 11 pm, respectively, relative to their equilibrium bond lengths.

As for dimethyl disulfide, stretching enhances the radical character of the atoms and groups in the stretched cystine backbone—in particular, of the sulfur atoms. The enhanced radical character affects reactivity, and we expect mechanical stretching to be particularly efficient in promoting radical reactions. Conversely, polar reactions are expected to be slowed down since the electrophilic/nucleophilic character of a reaction center decreases upon bond stretching. This is obviously a simplified picture, bearing in mind that reactivity is a consequence of simultaneous alterations of the radical and electrophilic/nucleophilic characters of all stretched groups and that the external force may stabilize or destabilize the transition state relative to the reactant by mechanochemical work.[39] As demonstrated by Beyer,[40] even a polar reaction rate can be mechanochemically enhanced.

The COGEF path of cystine spans the conformational range 90° ≤ θ ≤ 120°. This range may be narrowed when a cystine motif is locked within a biomolecular framework because of conformational hindrance—that is, whenever torsional motion is impeded by the backbone structure. Under an external load, a

Figure 4. Structure of the optimized (B3LYP/6-31G(d)) cystine molecule. The chiral carbon (C*) atoms are in β-position.

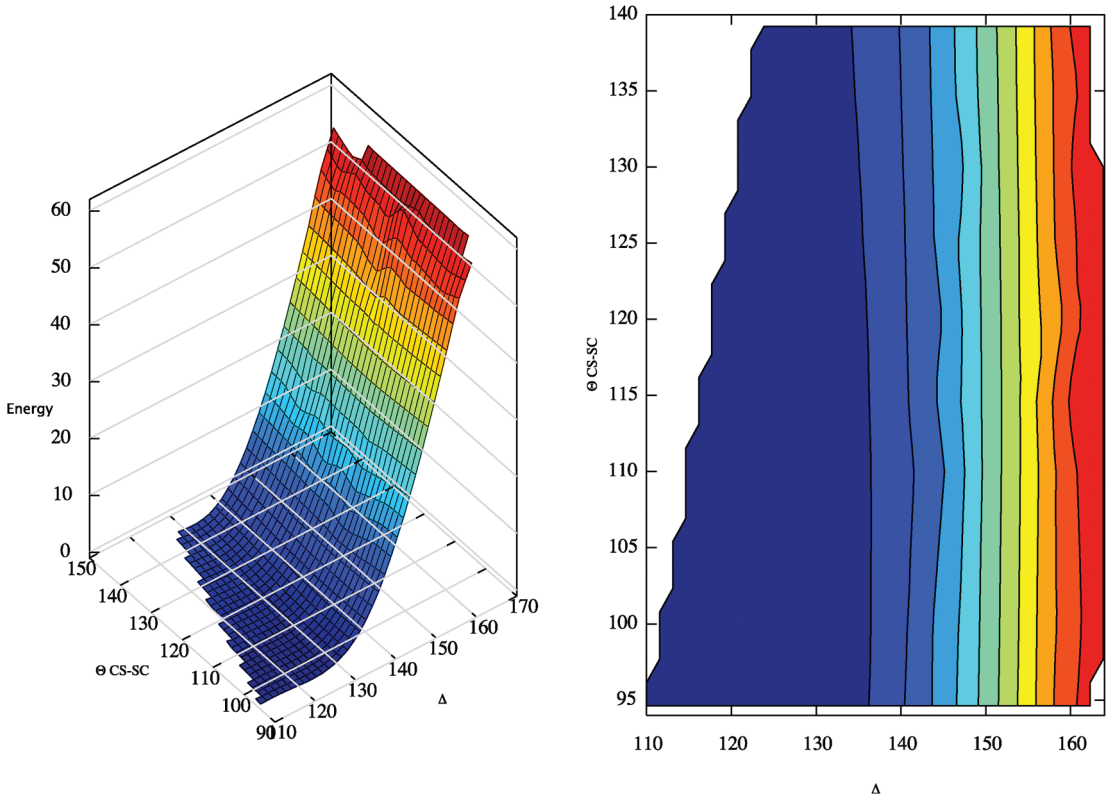

Figure 5. (Left) 2D-COGEF surface of the cystine: at each point, the molecular geometry has been optimized for fixed $\Delta_{C^*\leftrightarrow C^*}$ and θ. (Right) Corresponding isoenergy surface. The COGEF surface was computed at the UBP86/def2-SV(P) level of theory.

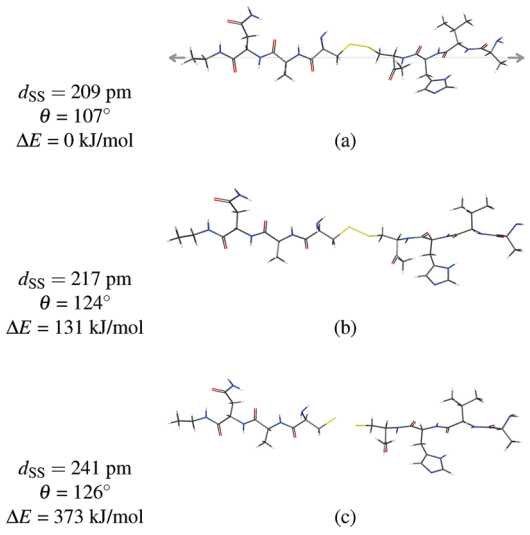

Figure 6. Stretching of titin-I27$_{SS}$ along the COGEF path at the B3LYP/6-31G(d) level of theory.

high torsional flexibility allows for a more efficient redistribution of the forces along the molecular backbone. To examine how the mechanochemistry is affected by a reduced torsional flexibility, we have computed a two-dimensional COGEF path by increasing (and constraining) θ as well as $\Delta_{C^*\leftrightarrow C^*}$, see Figure 5. Interestingly, the S−S bond length at the breaking point depends very little on the torsional angle. The mechanochemical strength of the disulfide bond thus does not depend strongly on conformational constraints.

Table 2. Mechanochemical Properties of the Disulfide Bond at the Breaking Point: the S−S Bond Length d_{SS}^b (pm), the Corresponding S−S Elongation Δ_{SS}^b (pm), the Torsional Angle θ^b (deg), the Rupture Force F_b (nN), the Elongation of the Attachment Points $\Delta_{X\leftrightarrow Y}$ (pm), and the Energy Relative to the Minimum $\Delta E^b = E^b - E^{eq}$ (kJ/mol) for Molecules of Increasing Size

UB3LYP/6-31G(d)	d_{SS}^b	Δ_{SS}	θ^b	Δ_θ	F_b	$\Delta_{X\leftrightarrow Y}$	ΔE^b	$F\cdot\Delta x^a$
CH_3SSCH_3	244.1	35.9	125	38	3.5	164.0	179	135
cystine	242.6	33.6	120	30	3.5	180.0	201	149
titin-I27SS	240.9	31.9	126	19	3.4	299.5	373	307

[a] F = force component along the bond elongation, Δx.

Titin Stretching. We have constructed a model of the titin I27 domain referred to as titin-I27$_{SS}$, consisting of 102 atoms with a central disulfide bridge, see Figure 6 and the Supporting Information. Its COGEF path was generated by applying the same elongation to each moiety of the backbone, thereby mimicking the effect of a constant load applied along the main axis. At each elongation, the structure was relaxed with respect to all degrees of freedom except the distance between the two carbon atoms at the two ends of the linear chain. Figure 6 shows snapshots of the COGEF path of titin-I27$_{SS}$.

The results for the three molecules are compared in Table 2. In all cases, the S−S bond is the weakest link. It ruptures at an elongation of more than 30 pm, which decreases slightly with increasing molecular size, while the breaking force decreases.

It is interesting to monitor the work $F\cdot\Delta x$ (where F is the force and Δx the elongation, see Table 2) done on the molecule during stretching. In the simulation, the force varies from zero to

the maximum value at the breaking point. At the breaking point, all bonds have undergone an elongation, which is more pronounced for the S−S bond (15.2%) and its neighboring S−C bonds (6.5%). The C−C, C−N, and N−CO bonds along the chain are elongated by 4.2%, 3.5%, and 2.7%, respectively, irrespective of their position in the chain. Upon stretching, the S−S bond accumulates 59.9 kJ/mol, whereas the neighboring S−C bonds accumulate 21.5 kJ/mol on average. The work done on the C−C, C−N, and N−CO bonds is 11.4, 9.3, and 7.0 kJ/mol, respectively. In total, the work done to elongate the chain bonds (306.7 kJ/mol) is less than the energy increase at the breaking point (ΔE^{b} = 373.0 kJ/mol). Hence, in the stretched system, about one-quarter of the energy is stored in modes other than bond stretching.

As already noted, force-induced stretching causes a reduction of the torsional flexibility of the molecular backbone. This loss of flexibility is expected to reduce the efficiency of those reactions that occur by a highly directional mechanism—that is, when the reactants must match a specific spatial configuration to enter the reactive channel. As we shall see below, one such reaction is the thiol−disulfide exchange.

Disulfide Cleavage Mechanism. The formal reduction

$$R{-}S{-}S{-}R' + 2H^{+} + 2e^{-} \rightleftharpoons R{-}S{-}H + R'{-}S{-}H$$

involves two protons and two electrons. In actual biological systems, disulfide bridge formation and cleavage occur by a thiol−disulfide exchange

$$R''{-}S{-}H + R{-}S{-}S{-}R' \rightleftharpoons R''{-}S{-}S{-}R + R'{-}S{-}H$$

which is essentially a nucleophilic S_N2 substitution reaction. In vivo, R″−S−H represents the thioredoxinenzyme, whereas in vitro it represents a suitable reagent—for example, ammonium thioglycolate (for the permanent wave), gluathinone, and dithiothreitol as well as related phosphine reagents and base catalysts have been observed for this reaction. As noted above, the effect of the force on the in vitro reaction has been studied by Fernandez et al.[11,16,17] By applying AFM in the force-clamp mode, these authors demonstrated that the resulting stretching force leads to protein unfolding and accelerates disulfide cleavage in the presence of a thiol or phosphine reagent. It has been observed that the reaction rate and possibly the reaction mechanism change with the strength of the applied force.

Based on the findings in the previous sections, we now analyze the S_N2 reaction corresponding to the cleavage of a protein disulfide bridge by the combined effect of external mechanical and chemical forces. For this purpose, we consider two different reaction models, the gas-phase model and the aqueous model, both studied at the UB3LYP/6-31G(d) level of theory.

Gas-Phase Model. This reaction involves a free anionic nucleophile:

$$\mathbf{CH_3S^-} + CH_3SSCH_3 \rightarrow \mathbf{CH_3S}SCH_3 + CH_3S^- \qquad (A)$$

The dimethyl disulfide molecule on the left mimics the protein disulfide bridge to be broken, whereas the free anion is a rough approximation to the nucleophile at a very high pH. This simple model is not expected to provide quantitative data but may still give physical insight.[39] It gives a barrierless reaction, the −S−S−S− adduct arrangement representing a minimum of 200 kJ/mol relative to the reactants, rather than a transition state as is typical for the −Y−C−X− arrangement of S_N2 reactions.[41] Since a perfectly symmetric arrangement of the three methyl groups is impossible, the two S−S bonds are different, with bond lengths 245 and 257 pm.

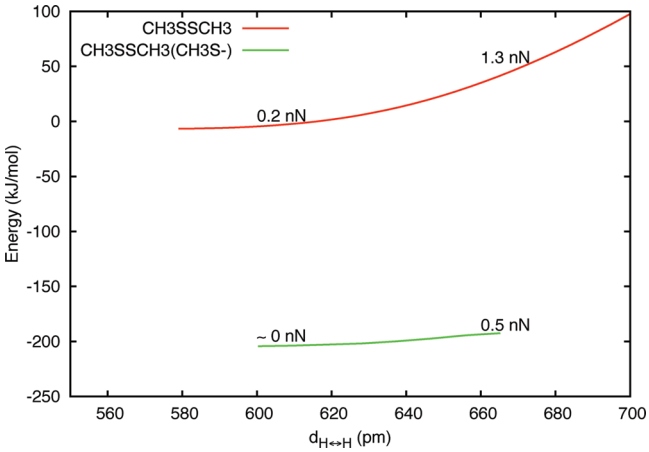

Figure 7. Adduct cluster $CH_3SSCH_3(CH_3S^-)$ (green curve) and isolated reactants CH_3SSCH_3 (red curve) for the reaction model A of the disulfide bond reduction, representing the gas-phase addition $\mathbf{CH_3S^-} + CH_3SSCH_3 \rightarrow \mathbf{CH_3S}SCH_3 + CH_3S^-$. The COGEF paths were computed using UB3LYP/6-31G(d) theory.

Figure 7 shows how the adduct (lower green curve) and the isolated dimethyl disulfide molecule (upper red curve) respond to a given amount of $d_{H\leftrightarrow H}$ stretching along the COGEF path. The restoring force is higher for the more tightly bonded dimethyl disulfide than for the looser adduct, leading to an increased stabilization of the adduct relative to the separated reactants with increased applied force. By stretching dimethyl disulfide in this manner, the effective force becomes well aligned with the central S−S bond. Although the force also affects other bonds, the general picture is that stretching of the molecule, including the S−S bond, leads to chemical activation. Despite the intuitive appeal of this simple model, the shortcomings of an idealized gas-phase model with a negative energy barrier are obvious. These ideas therefore need to be put to a more severe test.

Aqueous Model. The second model is more realistic in that it simulates an aqueous medium at physiological pH:

$$\mathbf{CH_3SH} + CH_3SSCH_3 \xrightarrow{H_2O} \mathbf{CH_3S}SCH_3 + CH_3\mathbf{SH} \qquad (B)$$

Four water molecules are included to model the surrounding medium, allowing both for solvation and for protolysis, in accordance with the Kohn−Sham studies by Fernandes and Ramos,[42] Bach et al.,[43] and Koti Ainavarapu et al.,[17] as discussed also by Aktah and Frank.[44] The reaction now has an energy barrier, in agreement with experimental observation. In the absence of an external force, the barrier height (without zero-point vibrational corrections) is 118 kJ mol^{-1}. This barrier is not associated with the S_N2 step per se (since the gas model has a inverse barrier) but arises from the deprotonation needed to make hydrogen sulfide a sufficiently strong nucleophile. Protolysis is accomplished by the water molecules and is synchronized with a concurrent protonation of the departing SCH_3 group by proton transfer through a hydrogen bond wire.[17] In other words, proton transfer occurs via the external water network, as one sulfur displaces another. While this model provides a realistic reaction mechanism, the computed activation energy is too high compared with the experimental estimate of about 60 kJ mol^{-1}.[45,46] Although

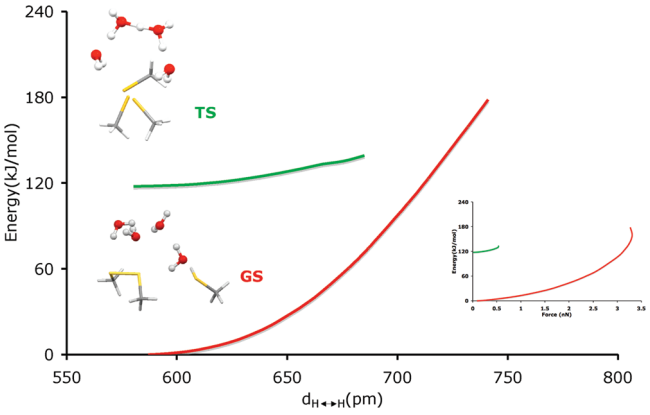

Figure 8. Reactants (RS, red curve) and transition structure (TS, green) for the reaction model B of the disulfide bond reduction, including four water molecules: $\mathbf{CH_3SH} + CH_3SSCH_3 \rightarrow \mathbf{CH_3SSCH_3} + CH_3\mathbf{SH}$. The COGEF paths were computed using UB3LYP/6-31G(d) theory.

the computed value is reduced by including a self-consistent reaction field,[17] only use of explicitly correlated ab initio methods in very large atomic basis sets are expected to provide quantitative agreement with experiment. In the present context, as already shown, the methods used are fully adequate.

Although we expect the S−S−S part of the reaction coordinate to respond to an external force in the same way as for the simpler gas-phase model, it is unclear how the network of water molecules will respond. The results of our COGEF calculations are displayed in Figure 8, which shows how the reactant and transition-state structures respond to the same applied displacement (main plot) and to the same applied force (inserted plot). At the onset, both energy curves are linear. Linearity persists through to $\Delta = 50$ pm and $F = 0.7$ nN. At longer elongations and higher forces, the red curve bends steeply up, and the energy difference between reactants and the transition state is drastically reduced. As a result of the stretching, the activation barrier decreases and the probability for the reaction to occur before the breaking point of the adduct increases. With regard to the chemical mechanism, the more advanced model provides a far more complex mechanism, the reaction coordinate at the transition state having a large component from the proton motion in the water part, see Figure 9. Clearly, the simple picture where the projection of this vector on the applied force determines the degree of activation cannot be applied.[17] On the other hand, it is gratifying that our model exhibits the correct mechanochemical behavior, in agreement with the experimental observation. We note that Koti Ainavarapu et al.[17] observed that reaction is promoted by stretching forces in the range 0.1−0.4 nN, well below the rupture force of the S−S bond and in the linear range of Figure 8.

The Modified Bell Formula. In mechanochemistry, it is customary to describe the observed kinetics by applying the Bell formula in the microcanonical formulation[47]

$$\kappa = Ae^{-(\Delta E^{\ddagger} - F\Delta x)/k_B T}$$

which is a variant of the Arrhenius equation. Here κ is the reaction rate, A is a constant, $\Delta E^{\ddagger}$ is the activation energy in the absence of the force F, and Δx is the distance to the transition state. The idealized Bell model is strictly valid only for simple one-dimensional bond-breaking processes rather than for more complicated chemical reactions, where the force may not be along the reaction coordinate. Within the realm of

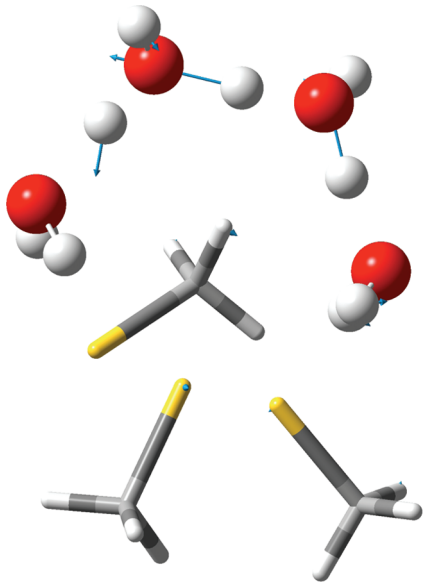

Figure 9. Displacement vectors along the reactive coordinate at the transition structure of the thiol−disulfide reaction.

transition-state theory and the Born−Oppenheimer approximation, a reactive event is represented by a trajectory in phase space passing through a critical configuration (transition structure), which is often approximated by the saddle point at the edge between the reactant and product valleys of the potential-energy surface. In this picture, only the transition and reactant states are relevant, the activation energy being determined by the energy difference between the two states.

In the aqueous reaction model B, the COGEFs of the transition and reactant states are linear at the onset (and their difference is constant), indicating that a constant force F can be applied in the Bell equation, although it is difficult to quantify the force and associated Δx value. As already observed, however, the linearity persists for a force smaller than 0.7 nN, beyond which the complex relationship between the variable multidimensionality of the reaction coordinate and the one-dimensionality of the force makes it impossible to apply the Bell formula quantitatively. On this basis, it becomes natural to propose a modified Bell formula that allows the two states to respond differently to an external mechanical force, taking into account the variation in the reaction coordinate from reactant to transition state. The model is obtained by replacing the finite-difference quantity $F\Delta x$ in the Bell formula by the integral difference

$$F\Delta x \rightsquigarrow \int_{\gamma,\mathrm{TS}} \vec{F}(\vec{r})\,\mathrm{d}\vec{s} - \int_{\gamma,\mathrm{RS}} \vec{F}(\vec{r})\,\mathrm{d}\vec{s}$$

where TS and RS denote the reactant and transition states, respectively, while γ is the integration path dictated by the experimental setup. Choosing the path to be the force-modified COGEF path ($\gamma = \mathcal{C}$), the modified Bell formula becomes

$$\kappa = Ae^{-(\Delta E^{\ddagger} - \Delta E^{\mathcal{C}})/k_B T} \quad \text{with}$$

$$\Delta E^{\mathcal{C}} = \int_{\mathcal{C},\mathrm{TS}} \vec{F}(\vec{r})\,\mathrm{d}\vec{s} - \int_{\mathcal{C},\mathrm{RS}} \vec{F}(\vec{r})\,\mathrm{d}\vec{s}$$

In simple terms, work carried out in directions other than the reaction coordinate is ineffective in promoting reaction.

dx.doi.org/10.1021/jp109428g |J. Phys. Chem. A 2011, 115, 2308–2315

CONCLUSIONS

The mechanochemistry of the disulfide bridge—that is, the influence of an external force on sulfur−sulfur bond cleavage, has been investigated by unrestricted Kohn−Sham theory. We have applied the COGEF (Constrained Geometry simulate External Force) approach to characterize the mechanochemical properties of the disulfide bond in three different chemical environments: CH_3SSCH_3, cystine, and a 102-atom molecule modeling the disulfide bridge in the I27 domain of the titin protein. At the UB3LYP/6-311++G(3df,3pd) level of theory, the CH_3SSCH_3 rupture force is 3.8 nN, corresponding to an S−S bond elongation of 35 pm.

Only small changes in the behavior of the S−S bond were observed with increasing system size, indicating that the interaction with neighboring atoms and the conformational rigidity of the protein environment have little influence on the mechanochemistry and validating the smallest system studied, dimethyl disulfide, as a representative model of the disulfide bridge, even in proteins. Upon stretching, the diradical character of the disulfide bridge increases, and the energy between the singlet ground state and low-lying triplet states decreases, suggesting that mechanical stretching is efficient at promoting radical reactions. The mechanism of the thiol−disulfide reduction reaction (in gas phase and water) under the effect of an external force was also investigated, by considering the COGEF potential for the adduct and the transition-state clusters. We observe that disulfide reduction is promoted by an external force in the range 0.1−0.4 nN, in qualitative agreement with experimental fits based on the Bell formula. However, the reaction coordinate is multidimensional, involving proton transfer assisted by water molecules. The simple Bell model can therefore only be applied in a qualitative manner. As a refinement, we propose a modified Bell formula that allows the two states to respond differently to the external force, taking into account the variation of the reaction coordinate from the reactant to transition state.

ASSOCIATED CONTENT

Supporting Information. Description of the molecular models and calibration of the methods used to compute ground-state properties and mechanochemical characteristics (Tables 1−4). This material is available free of charge via the Internet at http://pubs.acs.org.

AUTHOR INFORMATION

Corresponding Author

*E-mail m.f.iozzi@kjemi.uio.no.

ACKNOWLEDGMENT

The authors thank Prof. Julio M. Fernandez for the fruitful discussions and Dr. Lorna Dougan for the MD snapshot of the force-induced unfolded structure of the titin I27 domain. This work has received support from the Norwegian Research Council through a Centre of Excellence Grant (Grant No. 179568/V30), as well as through a grant of computer time from the Norwegian Supercomputing Program.

REFERENCES

(1) Berg, M.; Tymoczko, L.; Stryer, L. *Biochemistry*; W. H. Freeman: San Francisco, CA, 2007.
(2) Gilbert, F. *Methods Enzymol.* **1995**, *251*, 8–28.
(3) Beyer, M.; Clausen-Schaumann, H. *Chem. Rev.* **2005**, *105*, 2921–2946.
(4) Lee, S. W.; Jeong, G.; Campbell, E. *Nano Lett.* **2007**, *7*, 2590–2595.
(5) Puchner, E.; Gaub, H. *Curr. Opin. Struct. Biol.* **2009**, *19*, 605–614.
(6) Grandbois, M.; Beyer, M.; Rief, M.; Clausen-Schaumann, H.; Gaub, H. E. *Science* **1999**, *283*, 1727–1730.
(7) Kaupp, G. *Cryst. Eng. Commun.* **2009**, *11*, 388–403.
(8) Liang, J.; Fernandez, J. M. *ACS Nano* **2009**, *3*, 1628–1645.
(9) Rosen, B.; Percec, V. *Nature* **2007**, *446*, 381–382.
(10) Frank, I. *Angew. Chem., Int. Ed.* **2006**, *45*, 852–854.
(11) Wiita, A.; Perez-Jimenez, R.; Walther, K.; Grater, F.; Berne, B.; Holmgren, A.; Sanchez-Ruiz, J.; Fernandez, J. *Nature* **2007**, *450*, 124–127.
(12) Lu, H.; Schulten, K. *Biophys. J.* **2000**, *79*, 51–65.
(13) Dietz, H.; Berkemeier, F.; Bertz, M.; Rief, M. *Proc. Natl. Acad. Sci. U.S.A.* **2006**, *103*, 12724–12728.
(14) Ainavarapu, S.; Brujic, J.; Huang, H.; Wiita, A.; Lu, H.; Li, L.; Walther, K.; Carrion-Vazquez, M.; Li, H.; Fernandez, J. *Biophys. J.* **2007**, *92*, 225–233.
(15) Mickler, M.; Dima, R.; Dietz, H.; Hyeon, C.; Thirumalai, D.; Rief, M. *Proc. Natl. Acad. Sci. U.S.A.* **2007**, *104*, 20268.
(16) Wiita, A.; Ainavarapu, S.; Huang, H.; Fernandez, J. *Proc. Natl. Acad. Sci. U.S.A.* **2006**, *103*, 7222–7227.
(17) Ainavarapu, S. K.; Wiita, A.; Dougan, L.; Uggerud, E.; Fernandez, J. *J. Am. Chem. Soc.* **2008**, *130*, 6479–6487.
(18) Garcia-Manyes, S.; Liang, J.; Szoszkiewicz, R.; Kuo, T. *Nat. Chem.* **2009**, *1*, 236–242.
(19) Perez-Jimenez, R.; et al. *Nat. Struct. Mol. Biol.* **2009**, *16*, 890–896.
(20) Lu, H.; Schulten, K. *Chem. Phys.* **1999**, *247*, 141–153.
(21) Isralewitz, B.; Gao, M.; Schulten, K. *Curr. Opin. Struct. Biol.* **2001**, *11*, 224–230.
(22) Li, P.; Makarov, D. *J. Chem. Phys.* **2003**, *119*, 9260–9268.
(23) Dougan, L.; Koti, A.; Genchev, G.; Lu, H.; Fernandez, J. M. *Chem. Phys. Chem.* **2008**, *9*, 2836–2847.
(24) Beyer, M. *J. Chem. Phys.* **2000**, *112*, 7307–7312.
(25) Wolinski, K.; Baker, J. *Mol. Phys.* **2009**, *107*, 2403–2417.
(26) Ribas-Arino, J.; Shiga, M.; Marx, D. *Angew. Chem., Int. Ed.* **2009**, *48*, 4190–4193.
(27) Ribas-Arino, J.; Shiga, M.; Marx, D. *J. Am. Chem. Soc.* **2010**, *132*, 10609–10614.
(28) Ong, M. T.; Leiding, J.; Tao, H.; Virshup, A. M.; Martínez, T. J. *J. Am. Chem. Soc.* **2009**, *131*, 6377–6379.
(29) Lenhardt, J. M.; Ong, M. T.; Choe, R.; Evenhuis, C. R.; Martinez, T. J.; Craig, S. L. *Science* **2010**, *329*, 1057.
(30) Kucharski, T. J.; Huang, Z.; Yang, Q.-Z.; Tian, Y.; Rubin, N. C.; Concepcion, C. D.; Boulatov, R. *Angew. Chem., Int. Ed.* **2009**, *48*, 7040–7043.
(31) Iozzi, M. F.; Helgaker, T.; Uggerud, E. *Mol. Phys.* **2009**, *107*, 2537–2546.
(32) Weigend, F. *Phys. Chem. Chem. Phys.* **2002**, *4*, 4285.
(33) Frisch, M. J.; et al. *Gaussian 03*, revision C.02; Gaussian, Inc.: Wallingford, CT, 2004.
(34) TURBOMOLE V6.2 2010, a development of University of Karlsruhe and Forschungszentrum Karlsruhe GmbH, 1989−2007. TURBOMOLE GmbH, 2007.
(35) Minaev, B. F.; Ågren, H. *Collect. Czech. Chem. Commun.* **1995**, 60.
(36) Harvey, J. N.; Aschi, M.; Schwarz, H.; Koch, W. *Theor. Chem. Acc.* **1998**, *99*, 95–99.
(37) Øiestad, E. L.; Uggerud, E. *Int. J. Mass Spectrom.* **1999**, *185−187*, 231–240.
(38) Jarillo-Herrero, P. *Science* **2010**, *328*, 1362–1363.
(39) Krüger, D.; Rousseau, R.; Fuchs, H.; Marx, D. *Angew. Chem., Int. Ed.* **2003**, *42*, 2251–2253.
(40) Beyer, M. K. *Angew. Chem., Int. Ed.* **2003**, *42*, 4913–4915.
(41) Fernandez, I.; Frenking, G.; Uggerud, E. *Chem.—Eur. J.* **2009**, *15*, 2166–2175.

(42) Fernandes, P. A.; Ramos, M. J. *Chem.—Eur. J.* **2004**, *10*, 257–266.
(43) Bach, R. D.; Dmitrenko, O.; Thorpe, C. *J. Org. Chem.* **2008**, *73*, 12–21.
(44) Aktah, D.; Frank, I. *J. Am. Chem. Soc.* **2002**, *124*, 3402–3406.
(45) Rothwarf, D. M.; Scheraga, H. A. *Proc. Natl. Acad. Sci. U.S.A.* **1992**, *89*, 7944–7948.
(46) David, C.; Foley, S.; Mayon, C.; Enescu, M. *Biopolymers* **2008**, *89*, 623–634.
(47) Bell, G. *Science* **1978**, *200*, 618–627.